

***New Phytologist* Supporting Information**

Article title: Specific redox and iron homeostasis responses in the root tip of *Arabidopsis* upon zinc excess

Authors: Noémie Thiébaud, Manon Sarthou, Ludwig Richtmann, Daniel P. Persson, Alok Ranjan, Marie Schloesser, Stéphanie Boutet, Lucas Rezende, Stephan Clemens, Nathalie Verbruggen and Marc Hanikenne

Article acceptance date: 06 March 2025

The following Supporting Information is available for this article:

Fig. S1. Illustration of growth conditions and sampling of root tip and remaining roots for the RNA-Seq and ICP-MS analyses.

Fig. S2. Processing of Laser Ablation ICP-MS samples.

Fig. S3. Cell cycle synchronization analysis.

Fig. S4. Ionome profiling of the root tip and the remaining root system upon Zn excess in Arabidopsis.

Fig. S5. Partitioning of gene expression variation between root parts or between time-points.

Fig. S6. Gene Ontology enrichment analysis of genes regulated after 24h and 48h of Zn excess in RR of Arabidopsis.

Fig. S7. Gene Ontology enrichment analysis of genes regulated after 24h and 48h of Zn excess in RT of Arabidopsis.

Fig. S8. Gene Ontology enrichment analysis of genes regulated upon Zn excess in RR and RT of Arabidopsis.

Fig. S9. Impact of Zn excess on the expression of cell cycle phase, endocycle and DNA damage marker genes in Arabidopsis roots.

Fig. S10. Impact of Zn excess on differentiation in Arabidopsis roots.

Fig. S11. Normalization of the untargeted metabolomic profiling data.

Fig. S12. The camalexin biosynthetic pathway upon Zn excess in Arabidopsis roots.

Fig. S13. Primary root growth inhibition on *pad3* knocked-out mutants.

Fig. S14. Ionome profiling of the roots and shoots upon Zn excess and/or camalexin treatment in Arabidopsis.

Fig. S15. Expression of zinc and iron homeostasis genes in the *pad3-3* Arabidopsis mutant.

Fig. S16. Comparison of the impact of Zn excess and Cd stress on the metabolomic profile of the RT and RR in Arabidopsis.

Fig. S17. *PAD3* gene expression upon Fe deficiency in Arabidopsis.

Fig. S18. Primary root growth inhibition by Zn and Fe excesses in the Arabidopsis *pad3-3* mutant.

Table S1. Primers used for the RT-qPCR experiments.

Table S2. Genes presenting a higher or lower expression in RT than in RR, in control conditions and after 48h of Zn excess.

Table S3. Differentially expressed genes upon Zn excess in RT or RR, after 24h or 48h exposure to 200 μ M Zn.

Table S4. Gene Ontology enrichment analysis amongst the differentially expressed genes upon Zn excess (24h and/or 48h) in RT and RR.

Table S5. Impact of Zn excess on developmental processes in the RT.

Table S6. Differentially expressed genes upon Zn excess annotated with nutrient stress, signaling or transport GOs.

Table S7. Metabolomic analysis of root samples (RR and RT) in control conditions and after 48h of Zn excess.

Methods S1. This section presents detailed Materials and Methods.

Figure S1. Illustration of growth conditions and sampling of root tip and remaining roots for the RNA-Seq and ICP-MS analyses. **a.** Arabidopsis seeds sown on nylon mesh in a vertical plate. **b.** Germinated seedlings on the nylon mesh. **c.** Nylon mesh and seedling transfer to fresh media. **d.** On agar plate microdissection of the Root Tip (RT). **e.** Freshly cut RT on the agar plate. **f.** Remaining root after RT collection on agar media.

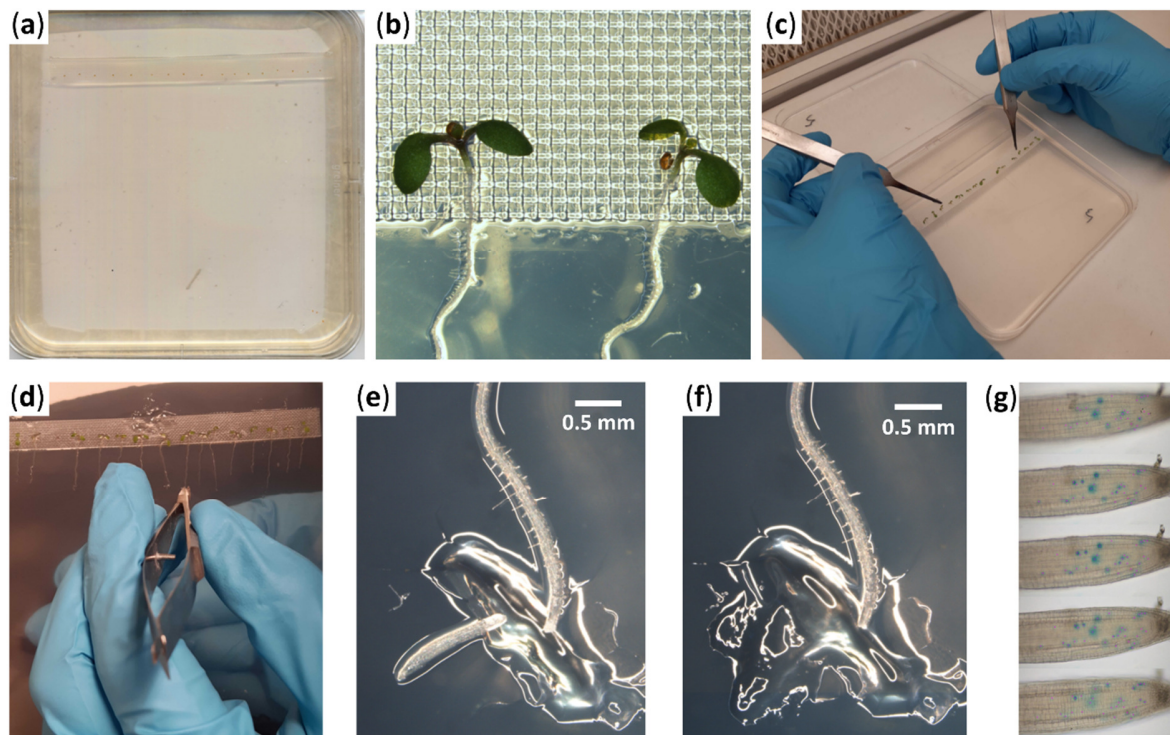


Figure S2. Processing of Laser Ablation ICP-MS samples. a-b. Microscopic pictures of bouquet sections of *Arabidopsis* differentiated roots (a) and RAM (b) samples embedded in paraffin. **c.** Representative potassium ^{39}K signal, used as a control, in differentiated root and RAM bouquets. **d-e.** Illustration of signal intensity collection within a region on interest, marked by a rectangle, across differentiated roots (d) and RAM (e). **f.** ^{39}K signal in differentiated roots (RR) and RAM (RT) bouquets. Each graph contains data for 8 differentiated root or RAM sections per condition, coming from two distinct root bouquets (see Methods S1 for details).

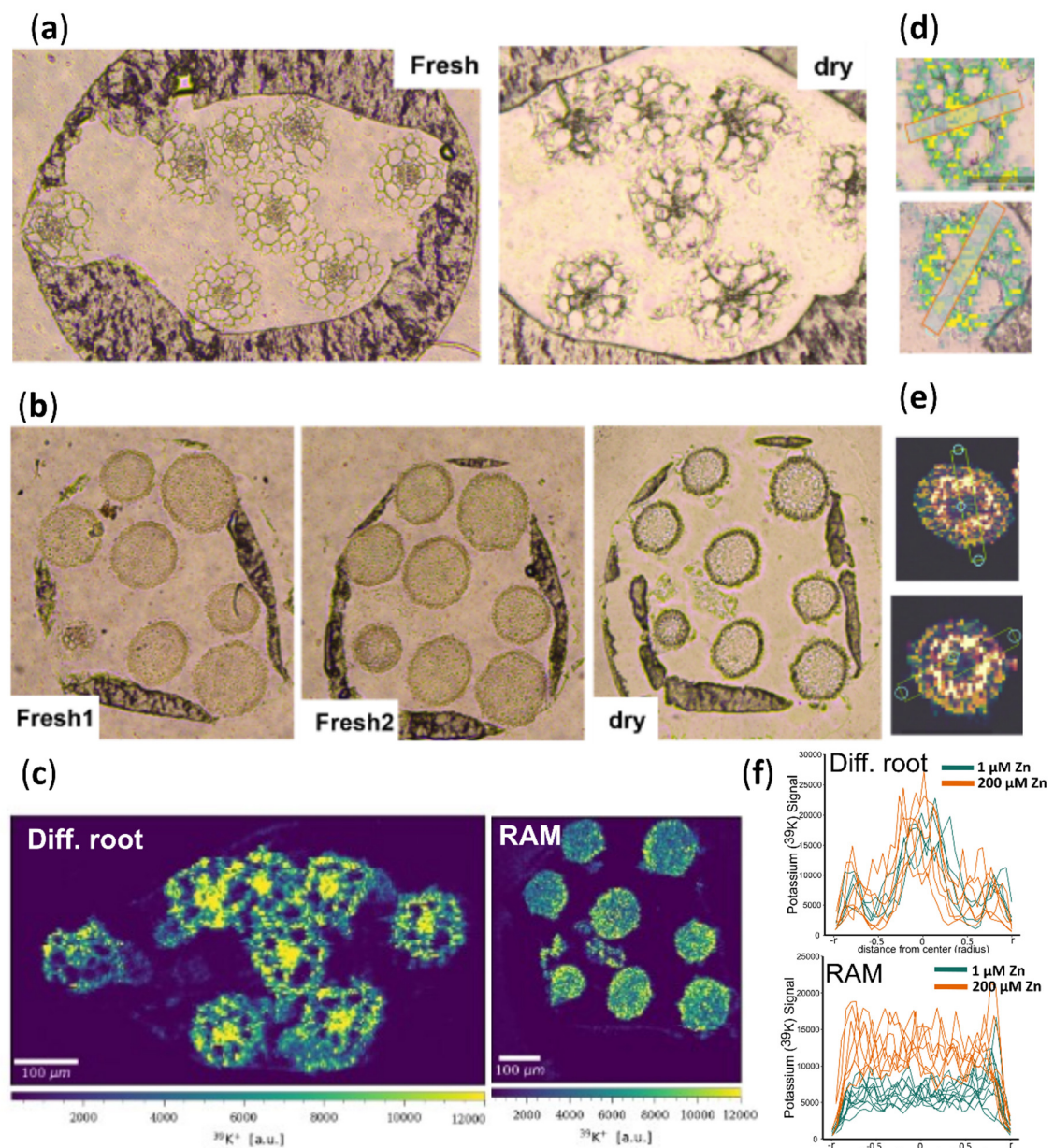


Figure S3. Cell cycle synchronization analysis. Cell cycle marker gene expression was synchronized with 2mM hydroxyurea in two-weeks old *Arabidopsis* seedlings exposed to control conditions (1 μ M) or treatment [1 week to control then 1 week to Zn excess (150 μ M Zn)]. **a-b.** pCYCA3;1:CYCA3;1:GUS seedlings were stained 0 h, 4 h, 8 h, 12 h, 16 h, 20 h, 22 h or 25 h after synchronization in control conditions (**a**) or Zn excess (**b**). **c-d.** pCYCB1;2:CYCB1;2:GUS seedlings were stained 0 h, 4 h, 8 h, 12 h, 16 h, 20 h, 22 h or 25 h after synchronization in control conditions (**c**) or Zn excess (**d**). **e-f.** GUS activity in pCYCB1;2:CYCB1;2:GUS was assessed by dot counting (Perilli & Sabatini, 2010) in the experiment represented in **a-d** (**e**) and an independent replicate experiment (**f**). Stars correspond to significantly different values (ANOVA type I). The experiments were carried out on 5 seedlings per condition per time-point.

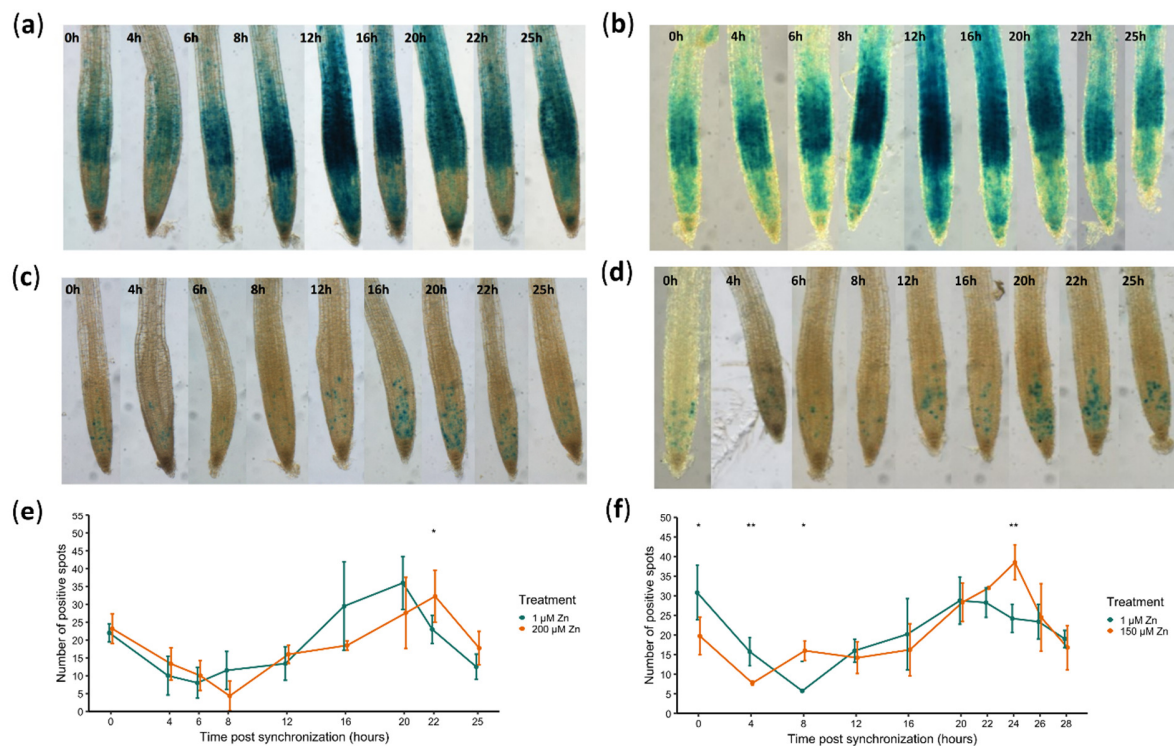


Figure S4. Ionome profiling of the root tip and the remaining root system upon Zn excess in *Arabidopsis*. Seedlings were germinated and grown for one week in control agar plates (1 μM Zn), then transferred for 24h or 48h onto new control or Zn excess (200 μM Zn) plates. Root tip (RT) and remaining root (RR) samples were then analyzed by ICP-MS. B, Ca, Cu, Fe, K, Mg, Mn, Ni and P concentrations are presented. Individual values are from three independent replicates. Each replicate consisted of a pool of dissected tissues from 750-870 seedlings. Different letters correspond to significantly different groups (ANOVA type I, with Tukey test correction, p-value < 0.05).

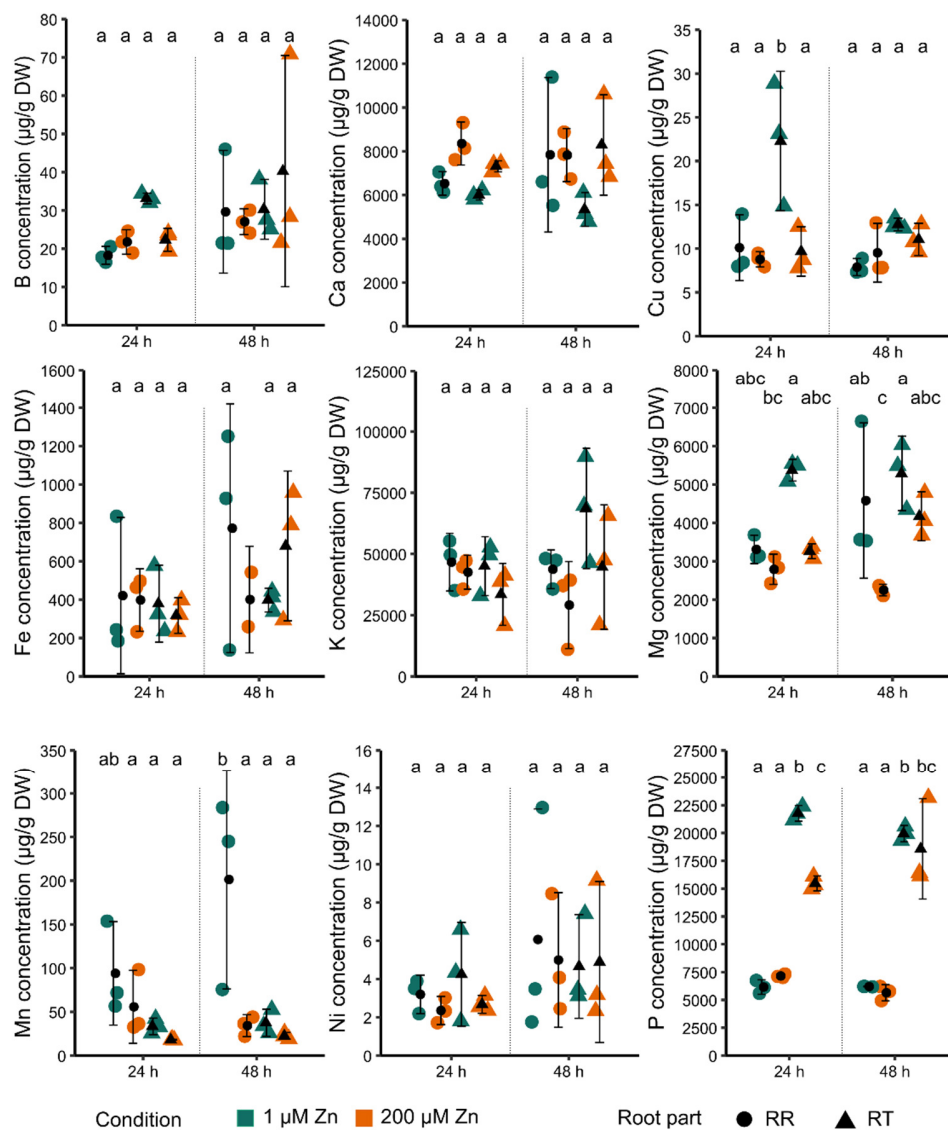


Figure S5. Partitioning of gene expression variation between root parts or between time-points. Arabidopsis seedlings were germinated and grown for one week in control agar plates (1 μ M Zn), then transferred for 24h or 48h onto new control or Zn excess (200 μ M Zn) plates. Root tip (RT) and remaining root (RR) samples were then submitted to RNA-Seq. **a.** Number of DEGs between RT and RR in control and/or in Zn excess conditions. **b-c.** Number of genes down-regulated in RR (**b**) and in RT (**c**) after 24h and 48h Zn excess. **d-e.** Number of genes up-regulated in RR (**d**) and in RT (**e**) after 24h and 48h Zn excess. Differentially expressed genes (DEG) between control and Zn excess conditions were identified separately for the 24h and 48h time points, with the following criteria: \log_2 (fold change) < -1 or > 1; adjusted *p-value* < 0.05.

(a)

	Higher in RT than RR	Lower in RT than RR	Sum higher and lower expression
Only at 1 μ M Zn	367	1129	1496
At 1 and 200 μ M Zn	959	3415	4374
Only at 200 μ M Zn	344	251	595
Total	1670	4795	

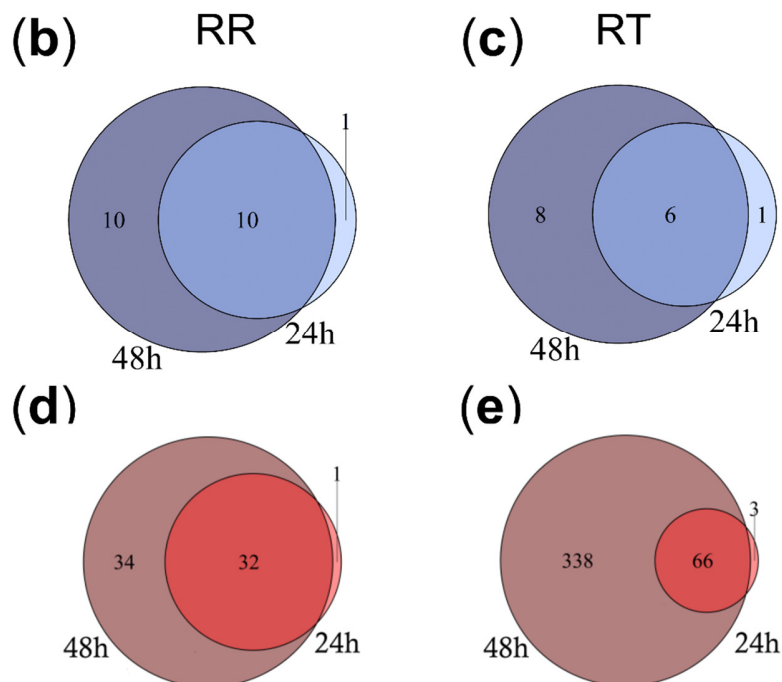
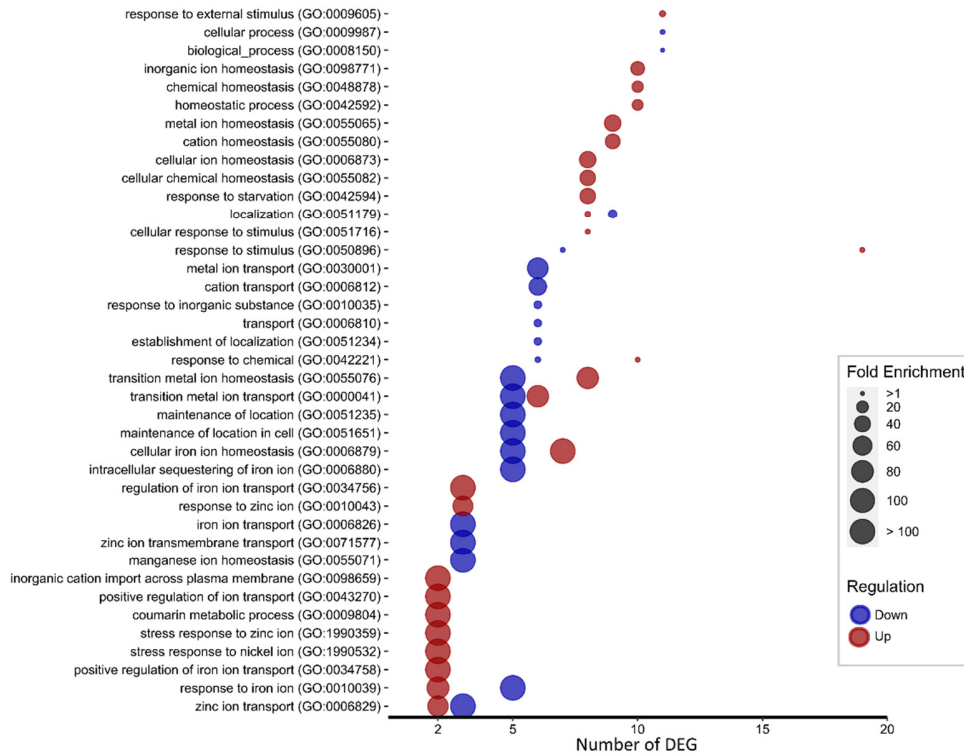


Figure S6. Gene Ontology (GO) enrichment analysis of genes regulated after 24h (top panel) and 48h (bottom panel) of Zn excess (200 μ M Zn) in remaining roots (RR) of Arabidopsis. Arabidopsis seedlings were germinated and grown for one week in control agar plates (1 μ M Zn), then transferred for 24h or 48h onto new control or Zn excess (200 μ M Zn) plates. Root tip (RT) and remaining root (RR) samples were then submitted to RNA-Seq. The top 15 GO for fold enrichment among genes that are up- or down-regulated by Zn excess in RR are represented in each panel. Complete data are presented in Table S4.

Remaining Roots GO term enrichment analysis

DEG at 24 h treatment (200 μ M Zn)



DEG at 48 h treatment (200 μ M Zn)

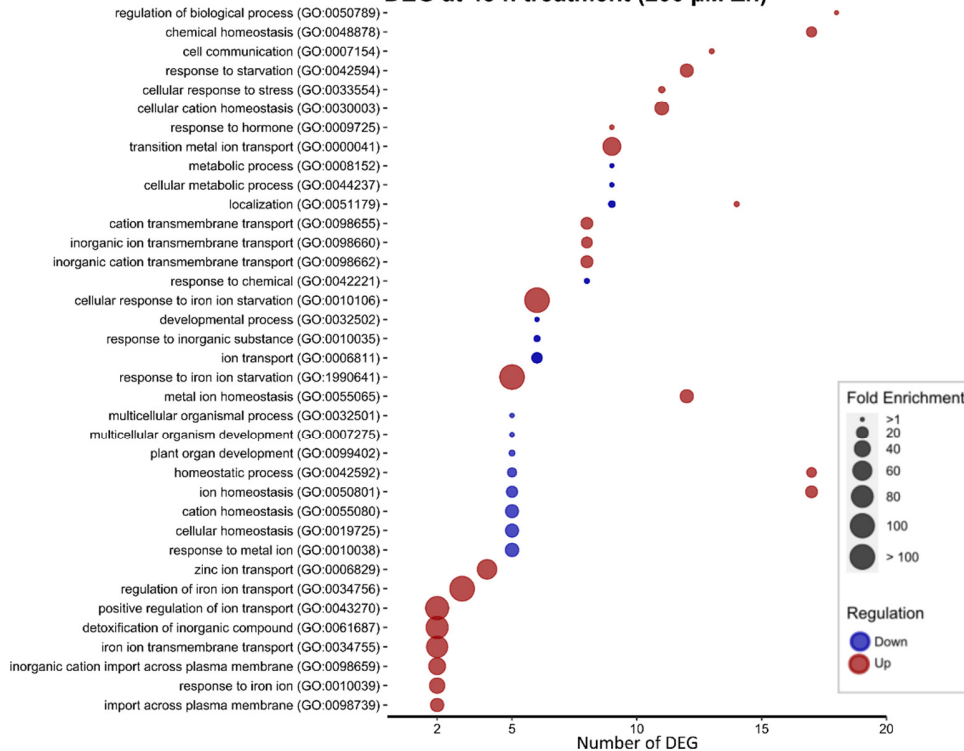


Figure S7. Gene Ontology (GO) enrichment analysis of genes regulated after 24h (top panel) and 48h (bottom panel) of Zn excess (200 μ M Zn) in root tips (RT) of Arabidopsis. Arabidopsis seedlings were germinated and grown for one week in control agar plates (1 μ M Zn), then transferred for 24h or 48h onto new control or Zn excess (200 μ M Zn) plates. Root tip (RT) and remaining root (RR) samples were then submitted to RNA-Seq. The top 15 GO for fold enrichment among genes that are up- or down-regulated by Zn excess in RT are represented in each panel. Complete data are presented in Table S4.

Root tips

GO term enrichment analysis

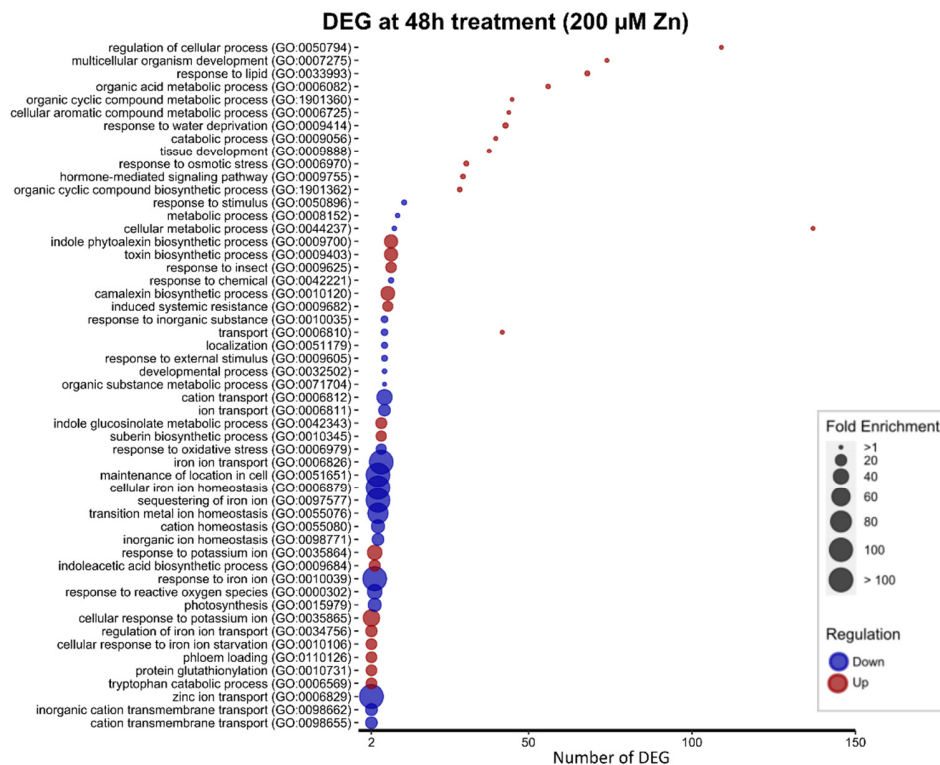
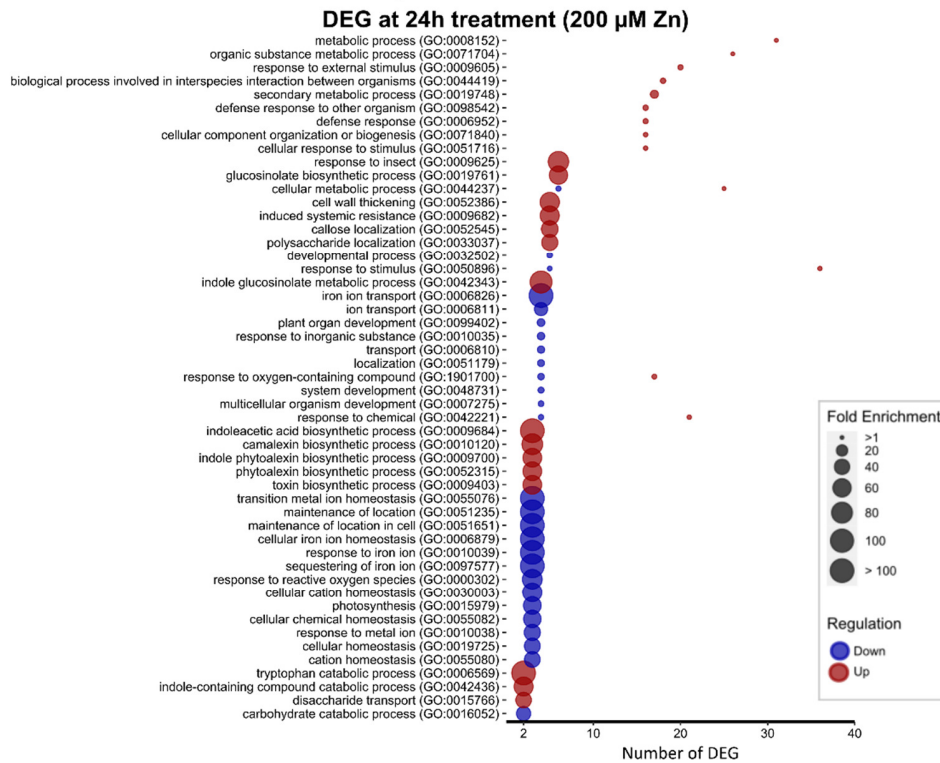
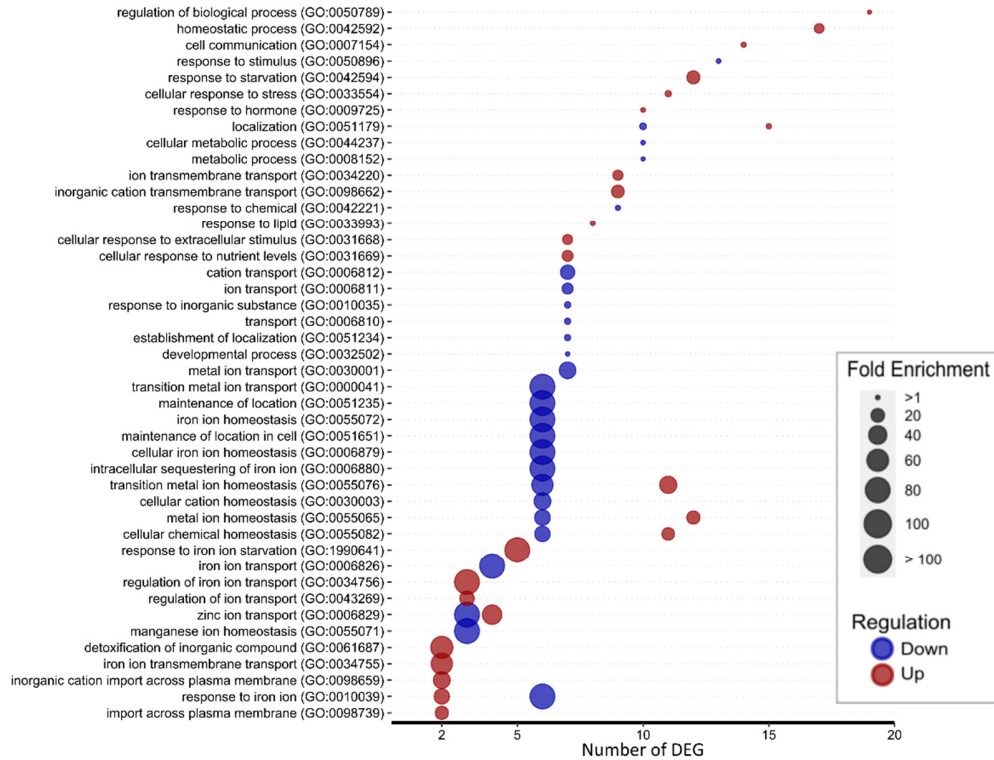


Figure S8. Gene Ontology (GO) enrichment analysis of genes regulated upon Zn excess (200 μ M Zn) in remaining roots (RR, top) and root tips (RT, bottom) of Arabidopsis. Arabidopsis seedlings were germinated and grown for one week in control agar plates (1 μ M Zn), then transferred for 24h or 48h onto new control or Zn excess (200 μ M Zn) plates. Root tip (RT) and remaining root (RR) samples were then submitted to RNA-Seq. DEGs identified after 24h and 48h of Zn excess were pooled prior analysis. The top 15 GO for fold enrichment among genes that are up- or down-regulated by Zn excess are represented in each panel. Complete data are presented in Table S4.

GO term enrichment analysis

DEG in the Remaining Roots (RR)



DEG in the Root Tips (RT)

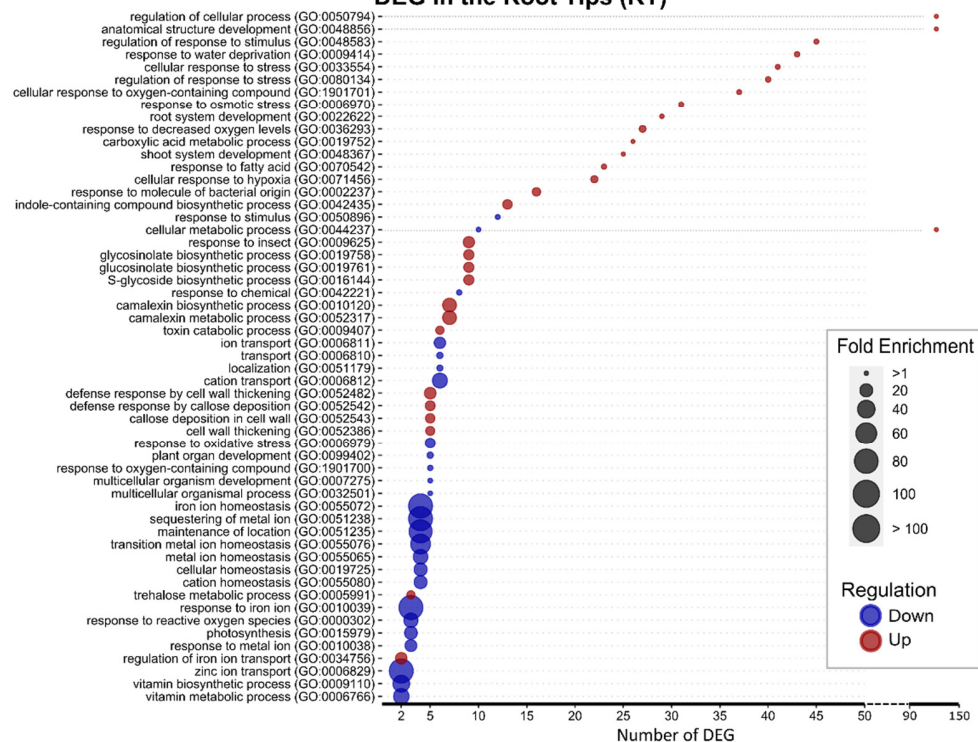


Figure S9. Impact of Zn excess on the expression of cell cycle phase, endocycle and DNA damage marker genes in Arabidopsis roots. Heatmap of $\log_2(\text{fold change})$ of gene expression between Zn excess (Zn+) and control conditions ($\text{DEG}_{\text{Zn+}/\text{Ctrl}}$) or between RT and RR ($\text{DEG}_{\text{RT}/\text{RR}}$), based on RNA-Seq data. Statistically-significant changes in gene expression (adjusted $p\text{-value} < 0.05$) are marked with stars : " * " for $p\text{-value} < 0.05$, " ** " for $p\text{-value} < 0.01$, " *** " for $p\text{-value} < 0.001$, " **** " for $p\text{-value} < 0.0001$.

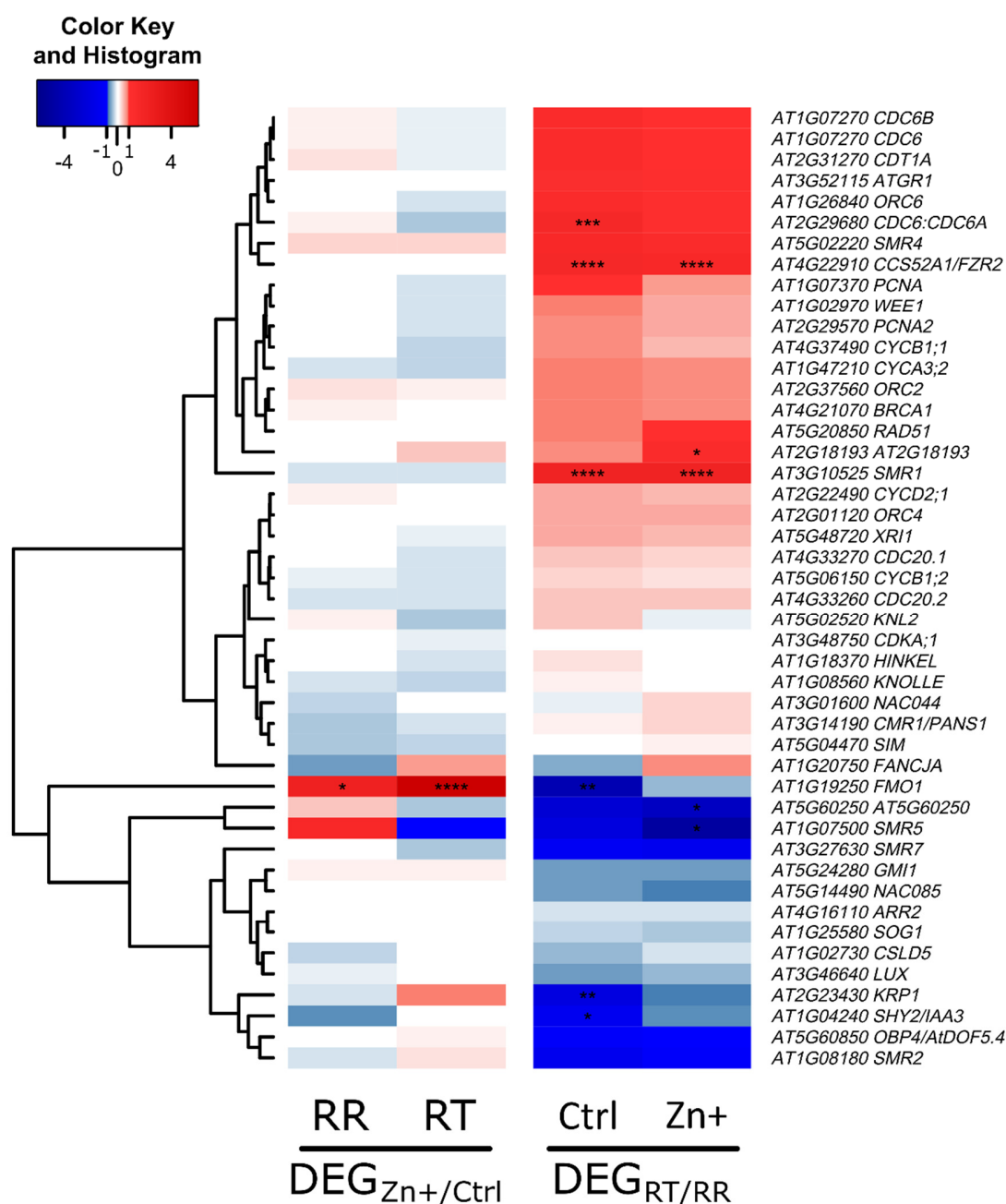


Figure S10. Impact of Zn excess on differentiation in Arabidopsis roots. Progression of the differentiation in the root tips upon Zn excess. Bulk RNA-Seq data from root tip (RT) and remaining root (RR) samples upon growth in control (1 μ M Zn) or Zn excess (200 μ M Zn, 48h) conditions were cross-referenced with the cell-type specific description of gene expression in roots provided by Shahan *et al.*, (2022). The figure shows the number of genes differentially expressed (upregulated \log_2 fold change > 1, downregulated \log_2 fold change < -1, adjusted p -value < 0.05) between excess and control conditions (Zn/control) in RT and RR that are among the 50 genes that are specific markers for each cell line and development stage.

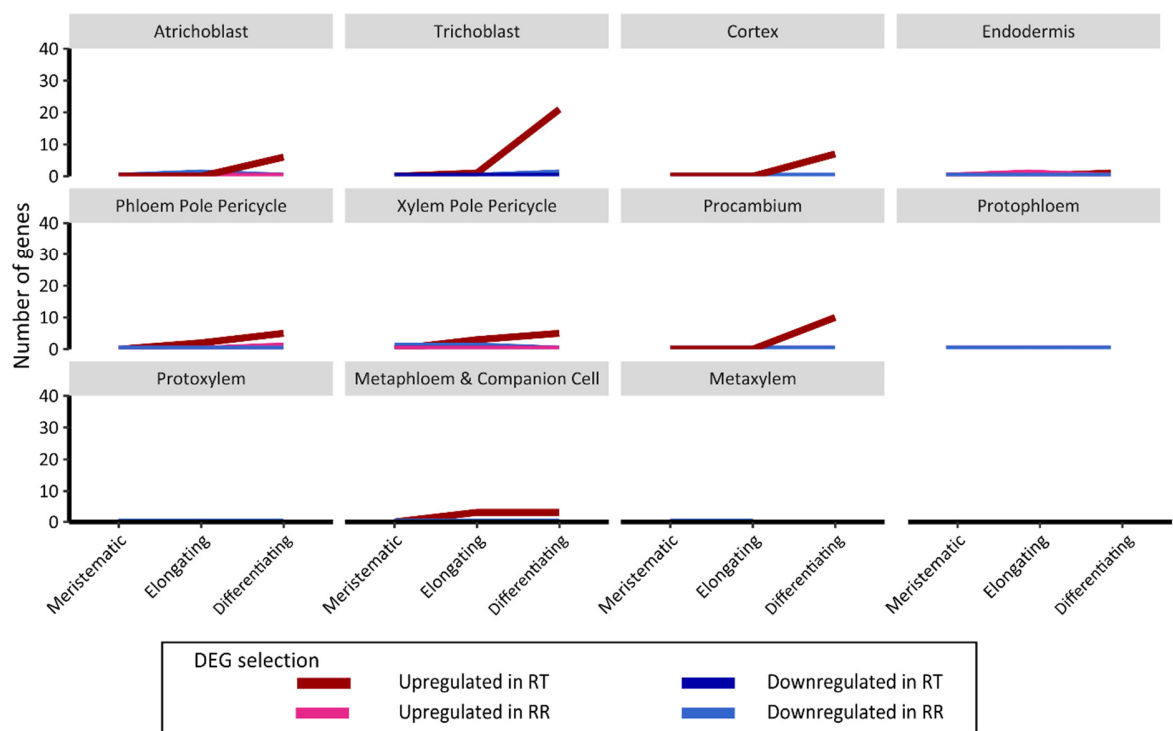


Figure S11. Normalization of the untargeted metabolomic profiling data. Arabidopsis seedlings were germinated and grown for one week in control agar plates (1 μM Zn), then transferred for 48h onto new control (1 μM Zn) or Zn excess (200 μM Zn) plates. Root tip (RT) and remaining root (RR, ~ 2 mm segment \sim mid-length of the root) samples were then submitted to untargeted metabolomic. **a.** Principal Component Analysis of the metabolomic data normalized according to the number of root pieces collected in each sample. **b.** Total metabolite abundance in RR and RT samples.

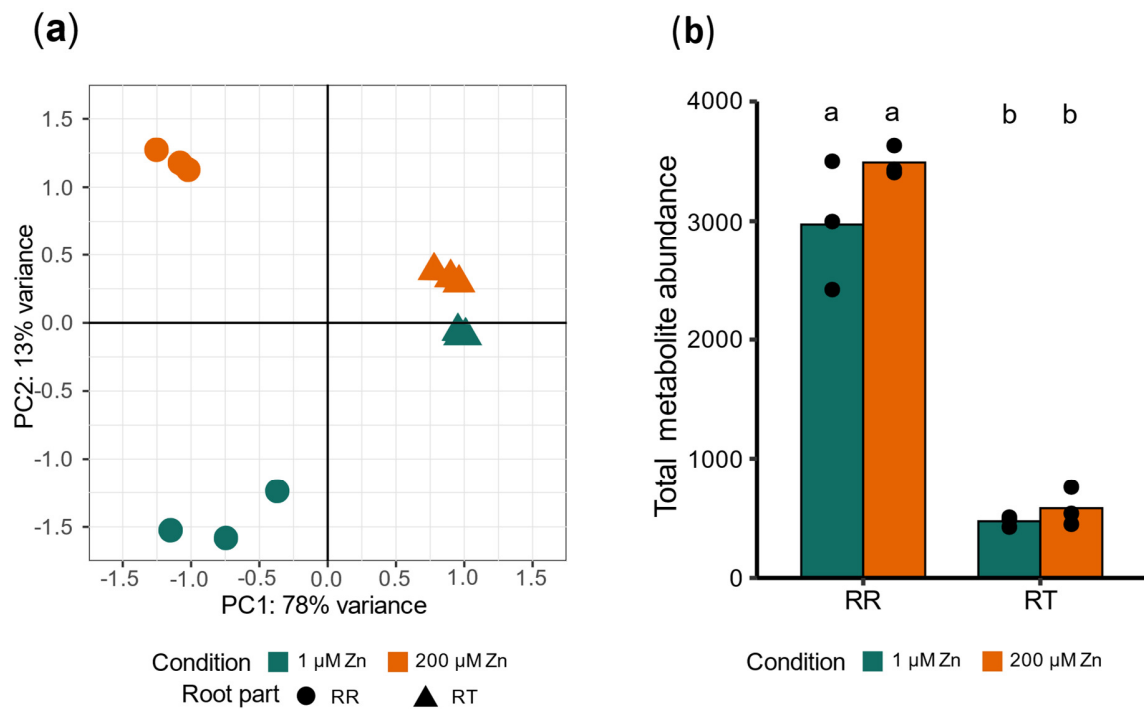


Figure S12. The camalexin biosynthetic pathway upon Zn excess in Arabidopsis roots.

References: [1] (Mucha *et al.*, 2019), [2] (Pfalz *et al.*, 2011, 2016), [3] (Hornbacher *et al.*, 2022), [4] (Böttcher *et al.*, 2014), [5] (Nafisi *et al.*, 2007), [6] (Rajniak *et al.*, 2015), [7] (Mikkelsen *et al.*, 2004), [8] (Sønderby *et al.*, 2010), [9] (Böttcher *et al.*, 2009), [10] (Kriechbaumer *et al.*, 2012), [11] (Pastorczyk *et al.*, 2020).

Figure S13. Primary root growth inhibition on *pad3* knocked-out mutants. **a.** Primary root growth of the *pad3-1* Arabidopsis mutant upon Zn excess. Seedlings were germinated and grown for one week in control agar plates (1 μ M Zn), then transferred for another week onto new control or Zn excess (200 μ M Zn) plates. Values are from 3 biological replicates, each including 9 seedlings. **b-d.** Col-0 and 3 different *pad3* knocked-out mutant seedlings were germinated and grown for 11 days on control (1 μ M Zn) or Zn excess (75 μ M Zn) agar plates. **b.** Representative pictures of 11 day-old seedlings. **c.** Fresh weight (FW) of shoots and roots, relatively to the control treatment (1 μ M Zn). **d.** Primary root growth was measured after 11 days of growth, relative to their respective control condition, each sample included from 50 to 230 independent measurements. Different letters correspond to significantly different groups (ANOVA type I, with Tukey test correction, *p*-value < 0.05).

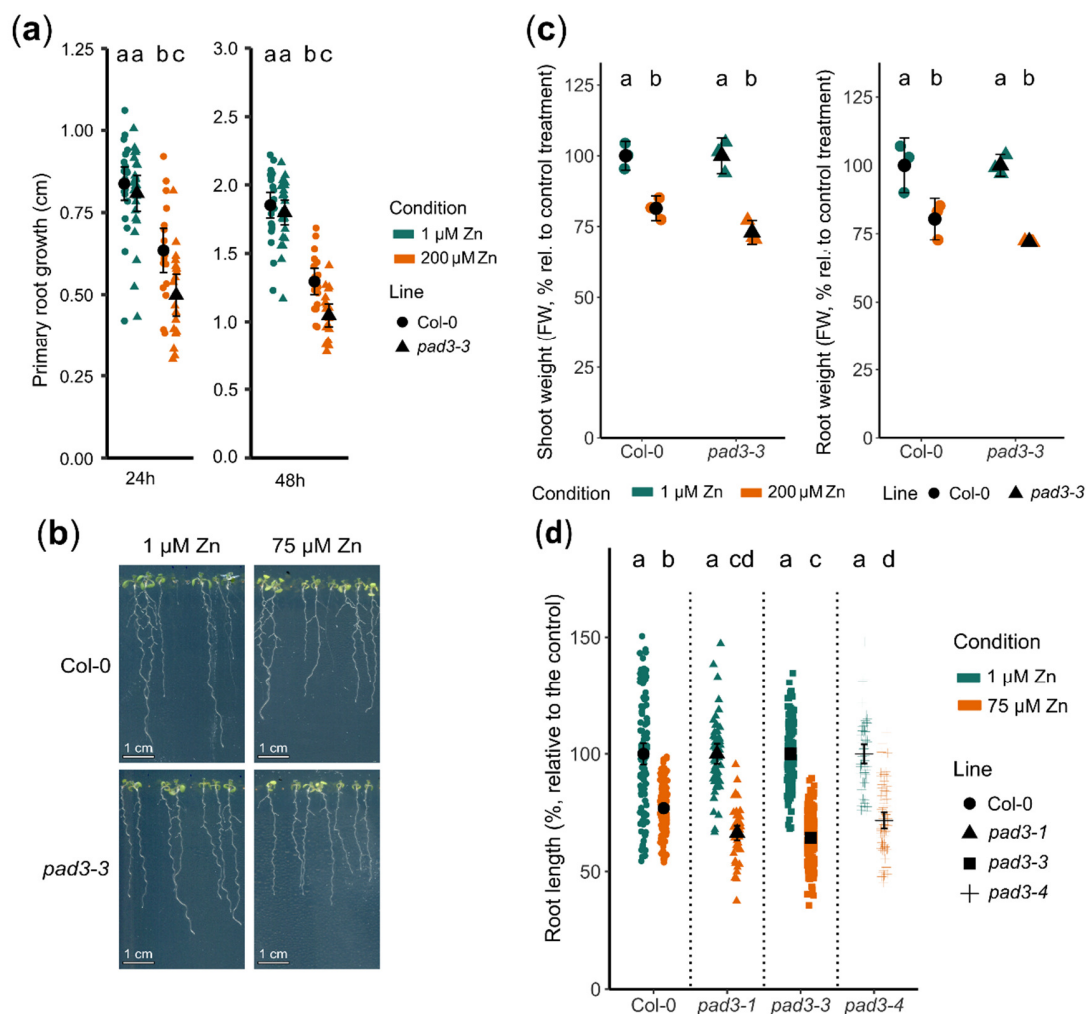
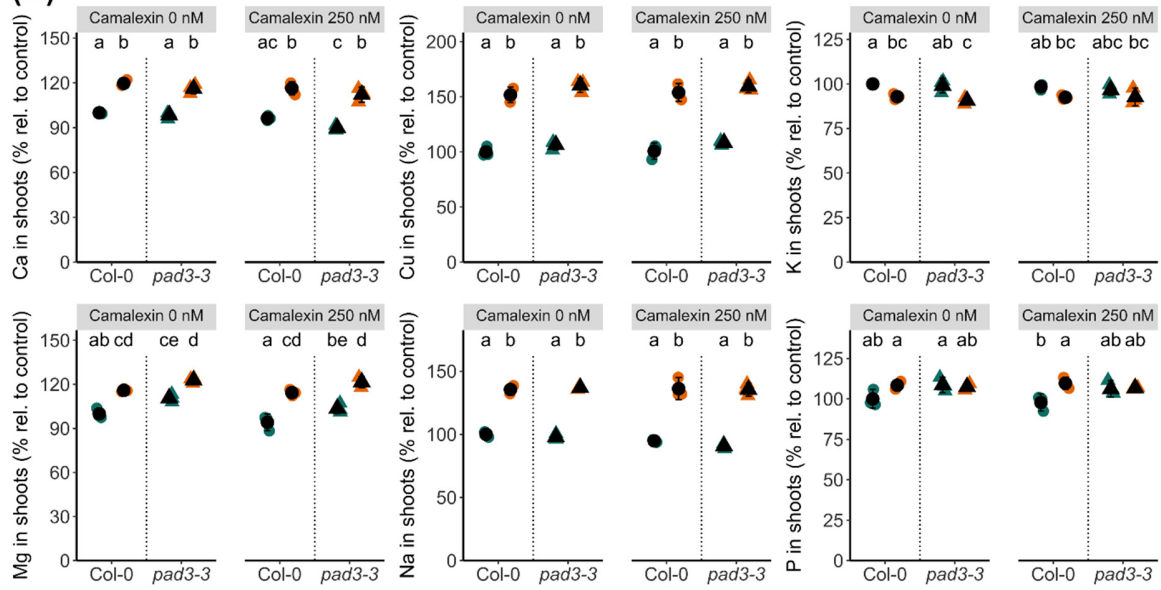
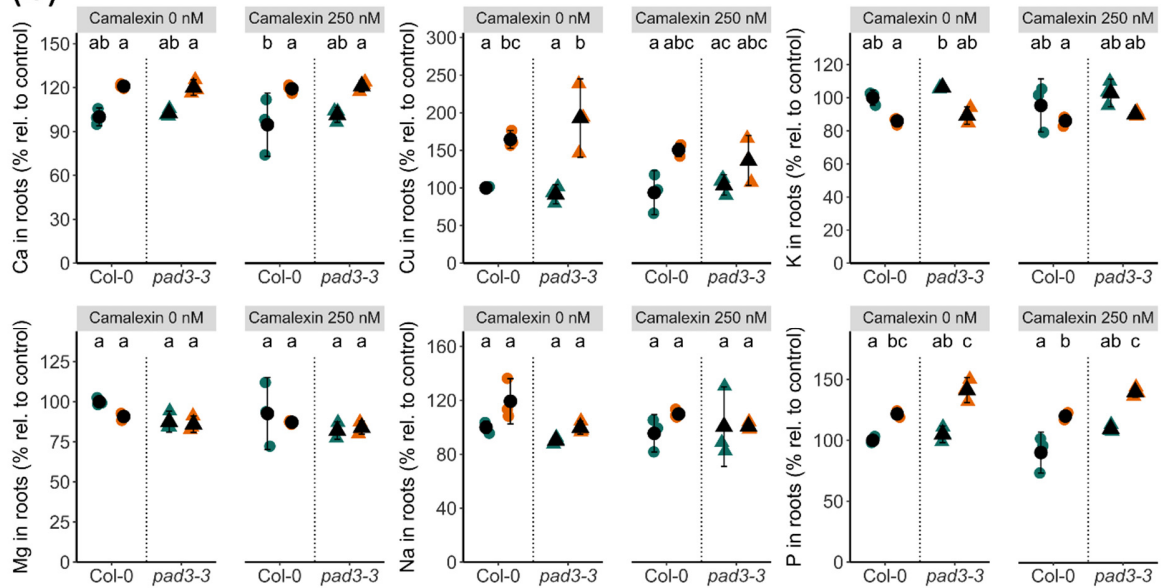


Figure S14. Ionome profiling of the roots and shoots upon Zn excess and/or camalexin treatment in Arabidopsis. Col-0 and *pad3-3* knocked-out mutant seedlings were germinated and grown for 11 days on control (1 μ M Zn) or Zn excess (75 μ M Zn) agar plates, and control (0 nM) or exogenous camalexin treatment (250 nM). Elemental concentrations are relative to their concentrations in Col-0 in control condition, from 3 biological replicates, each including 60 to 90 seedlings. Zn, Fe and Mn concentrations are presented in Fig. **7d**. Different letters correspond to significantly different groups (ANOVA type I, with Tukey test correction, *p-value* < 0.05).

(a)



(b)



Condition ■ 1 μ M Zn ■ 75 μ M Zn Lines ● Col-0 ▲ *pad3-3*

Figure S15. Expression of zinc and iron homeostasis genes in the *pad3-3* Arabidopsis mutant.

Col-0 and *pad3-3* knocked-out mutant seedlings were germinated and grown for 11 days on control (1 μ M Zn) or Zn excess (75 μ M Zn) agar plates. Gene expression was assessed by RT-qPCR and normalized over 3 reference genes. Data were obtained from 3 biological replicates (40-60 seedlings/replicate), each with 3 technical replicates. Different letters correspond to significantly different groups (ANOVA type I, with Tukey test correction, *p*-value < 0.05).

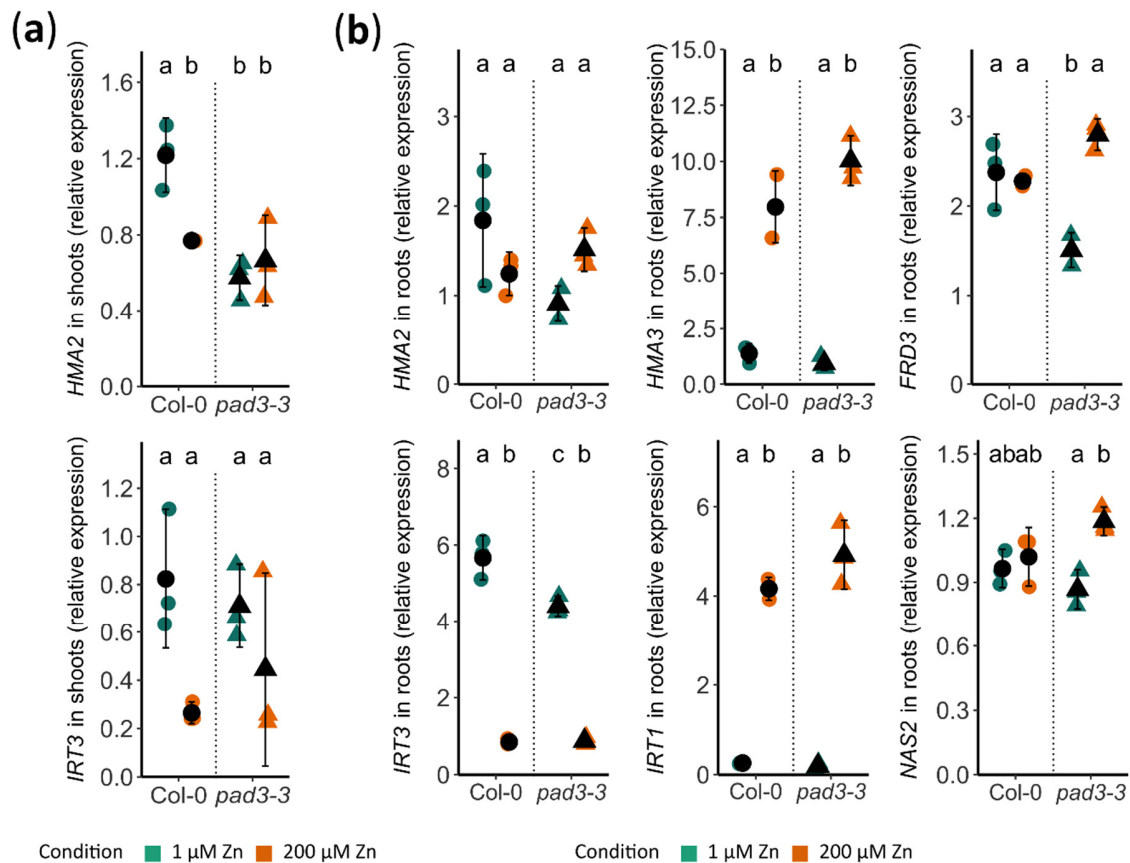


Figure S16. Comparison of the impact of Zn excess and Cd stress on the metabolomic profile of the root tip and the remaining root system in *Arabidopsis*. Seedlings were germinated and grown for one week in control agar plates (1 μ M Zn), then transferred for 48h onto new control (1 μ M Zn), Zn excess (200 μ M Zn) or Cd (25 μ M) plates. Root tip (RT) and remaining root (RR, ~2 mm segment ~mid-length of the root) samples were then submitted to untargeted metabolomic. Data were normalized according to the total count features of the control sample, for each root part. Control, Zn excess and Cd stress experiments were simultaneously performed. The Cd stress data are described in details in (Richtmann *et al.*, 2024). DAF: Differentially Accumulated Features.

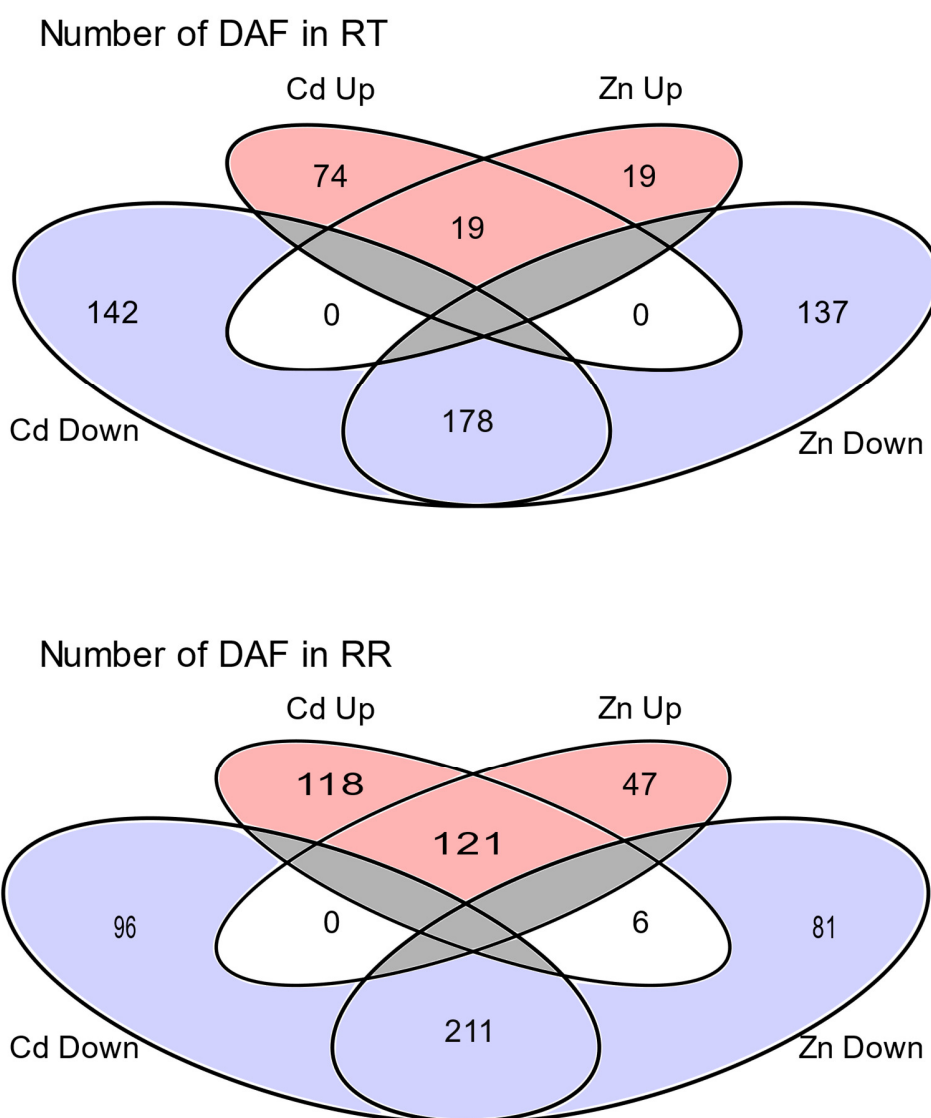


Figure S17. *PAD3* gene expression upon Fe deficiency in Arabidopsis. Col-0 plants were hydroponically grown for 3 weeks in control Hoagland medium, then transferred for 3 weeks in control medium (CM, 1 μ M Zn, 10 μ M Fe-HBED) or Fe depleted medium (1 μ M Zn, 0 μ M Fe). Gene expression was assessed by RT-qPCR and normalized over 2 reference genes. Data were obtained from 3 biological replicates (2-3 plants/replicate), each with 3 technical replicates. Different letters correspond to significantly different groups (ANOVA type I, with Tukey test correction, p -value < 0.05).

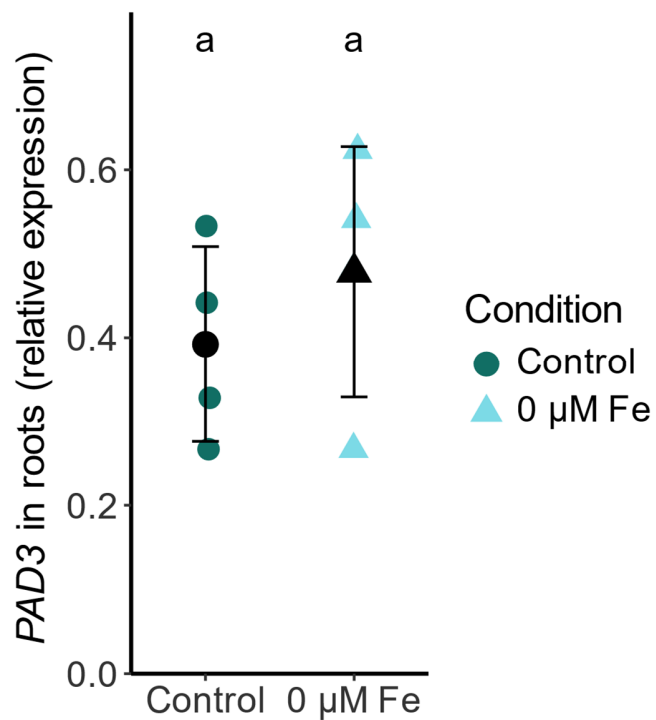
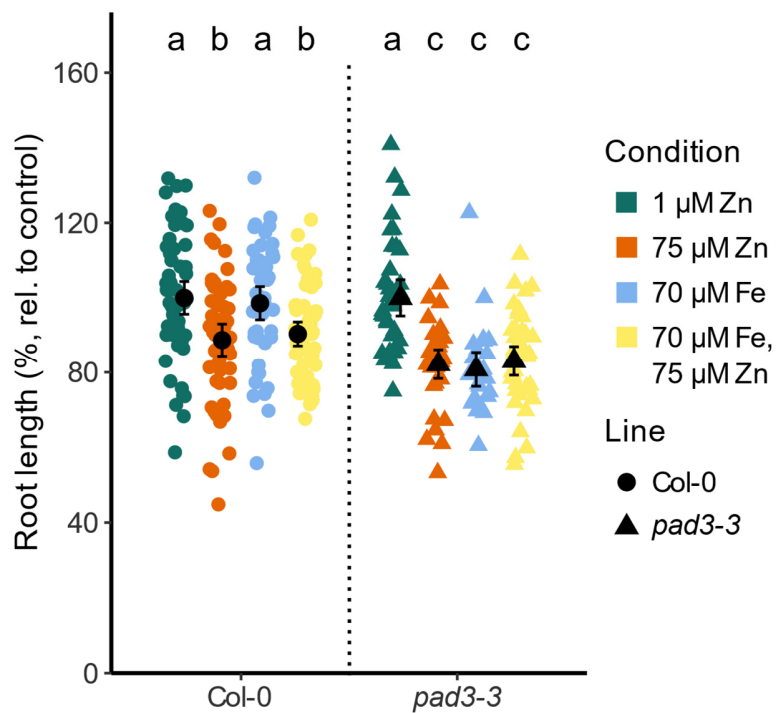


Figure S18. Primary root growth inhibition by Zn and Fe excesses in the *Arabidopsis pad3-3* mutant. Col-0 and *pad3-3* knocked-out mutant seedlings were germinated and grown for 11 days on control (1 μ M Zn), Zn excess (75 μ M Zn), Fe excess (70 μ M Fe) or Fe-Zn double excess (70 μ M Fe, 75 μ M Zn) agar plates. Primary root growth was measured after 11 days of growth, relative to their respective control condition, each sample included 30-60 independent measurements. Different letters correspond to significantly different groups (ANOVA type I, with Tukey test correction, p -value < 0.05).



Supporting Information Tables (Captions)

The data are available as independent Excel sheets.

Table S1. Primers used for the RT-qPCR experiments.

Table S2. Genes presenting a higher or lower expression in RT than in RR, in control conditions and after 48h of Zn excess.

Table S3. Differentially expressed genes upon Zn excess in RT or RR, after 24h or 48h exposure to 200 μ M Zn.

Table S4. Gene Ontology enrichment analysis amongst the differentially expressed genes upon Zn excess (24h and/or 48h) in RT and RR.

Table S5. Impact of Zn excess on developmental processes in the RT.

Table S6. Differentially expressed genes upon Zn excess annotated with nutrient stress, signaling or transport GOs.

Table S7. Metabolomic analysis of root samples (RR and RT) in control conditions and after 48h of Zn excess.

Methods S1

This section presents detailed Materials and Methods.

Plant material and growth conditions

Arabidopsis thaliana (L.) Heynh. (Col-0) was used in all experiments. The *pad3-1* (*phytoalexin deficient*, (Glazebrook *et al.*, 1997), *pad3-3* (SALK_026585C), *pad3-4* (SALKseq_059784.1), as well as the pCYCB1;2:CYCB1;2:GUS (N799897) and pCYCA3;1:CYCA3;1:GUS (N799893) lines, were obtained from NASC (Nottingham Arabidopsis Stock Centre) and used as homozygote lines.

Plants were grown vertically on agar plates with Hoagland medium [1.5 mM Ca(NO₃)₂, 0.28 mM KH₂PO₄, 0.75 mM MgSO₄, 1.25 mM KNO₃, 0.5 μM CuSO₄, 1 μM ZnSO₄, 5 μM MnSO₄, 25 μM H₃BO₃, 0.1 μM Na₂MoO₄, 50 μM KCl, 10 μM Fe-HBED, 3 mM MES, 1% (w/v) sucrose, 0.8 % (w/v) agar (M-type, Sigma), pH 5.7] in BrightBoy GroBanks (CLF Plant Climatics) under long day conditions (16 h light, 21°C, 100 μmol.m⁻².s⁻¹ / 8 h dark, 18°C). For the Laser Ablation ICP-MS experiment, seedlings were grown under slightly different conditions [16 h light, 22°C, 125 μmol.m⁻².s⁻¹ / 8 h dark, 20°C, in a Percival chamber (CLF Plant Climatics)].

Seeds were surface sterilized by rinsing 3 min with 70 % ethanol and 2 min with 2 % bleach. After 3 washing steps with sterile water, the seeds were suspended in 0,1 % (w/v) sterile agar. For most experiments, seeds were sown on control agar plates on nylon meshes (200 μm aperture, Prosep filters) and stratified (4°C, 2 days) (Fig. S1). After 7 days, seedlings were transferred to either new control plates (1 μM Zn) or Zn excess plates (200 μM Zn), and treated for 24 hours, 48 hours or 7 days (Fig. S1). The experimental design combining germination on control medium then transfer to a high Zn concentration (200 μM) was selected based on preliminary experiments, meeting several requirements: it enabled (i) initial seedling establishment in a non-toxic condition, reduced growth shortly after transfer, (ii) the capture of the initial changes in the root tip (RT) upon Zn exposure, (iii) survival of the seedlings. Note that for the analysis of cell cycle reporter lines, a Zn concentration of 150 μM Zn instead of 200 μM was used. For the *pad3* mutant characterization, seeds were sown directly on control (1 μM Zn) or treated (75 μM Zn) Hoagland media, supplemented or not with 250 nM of camalexin (Sigma Aldrich), and grown for 11 days. A camalexin concentration of 250 nM was selected as it corresponds to the concentration of camalexin in roots after 11 days of 75 μM Zn treatment, as determined in our targeted metabolomic approach. This simplified the handling of the experiments. Using lower Zn concentrations for a longer time achieved an overall similar growth reduction than in transfer experiments.

Growth assays under Fe-Zn excess conditions (Fig. **S17**) were carried out in the same conditions as for the other *pad3* mutant experiments, except that seedlings were grown on control (1 μ M Zn, 10 μ M Fe), or upon Fe (1 μ M Zn, 70 μ M Fe), Zn (75 μ M Zn, 10 μ M Fe) or Fe-Zn (75 μ M Zn, 70 μ M Fe) excesses.

Plants used for the RT-qPCR to investigate the effect of Fe deficiency on *PAD3* expression were hydroponically grown in control liquid Hoagland medium for 3 weeks (short days, 8h light, 22°C, 100 μ mol.m⁻².s⁻¹ / 16h dark, 20°C). They were then transferred for 3 weeks into control (10 μ M Fe) or treatment media (0 μ M Fe).

A description of the experimental replication levels is presented in each figure legend.

Root growth and RAM phenotyping

At three independent time-points (after the transfer to fresh plates at day 7, and after 24h and 48h of treatment), the root apex was marked at the back of the plate for root growth measurement (Fig. 1A). Plates were scanned with an EPSON V3300 scanner after 7 days of treatment and roots were measured with FIJI (<https://imagej.net/Fiji>). To measure the root apical meristem (RAM) size, seedlings treated for 24h and 48h were rinsed 30 seconds in distilled water, then stained in the dark for 2 minutes in propidium iodide (33.4 mg/L) and rinsed again in distilled water. Roots were mounted on glass slides and visualized with a SP2 TCS AOBS confocal laser-scanning inverted microscope (Leica, Mannheim, Germany) with excitation at 543 nm and emission between 600 and 730 nm. The pictures of the propidium iodide-stained roots were then used to quantify several morphological features using FIJI, as follows. The length of the meristematic zone was assessed as the distance between the first elongated cortex cell and the quiescent center (QC) (Perilli & Sabatini, 2010). The number of cortex cells in this zone was simultaneously assessed and a mean cortex cell size in RAM was calculated by dividing the length (in μ m) by the number of cortex cells for each root. To estimate the size of the elongation zone (EZ), the distance between the root apex and the first root hair was measured for each root.

Cell cycle analyses

Two-week-old seedlings exposed to control conditions (1 μ M) or treatment [1 week to control then 1 week to Zn excess (150 μ M Zn)] were harvested in cold acetone (90% v/v) and then incubated at room temperature for 20 min. Seedlings were rinsed in GUS staining buffer [0.2% Triton X-100, 2 mM Fe(CN)₆³⁻ (Ferrocyanide), 2 mM Fe(CN)₆⁴⁻ (Ferricyanide), 7.7 mM NaH₂PO₄ and 17.1 mM Na₂HPO₄] and vacuum-infiltrated with staining buffer in the presence of 5-bromo-4-chloro-3-indolyl- β -D-glucuronide (104.4 μ g/mL, X-Gluc) until sinking of the seedlings. The staining reaction was then conducted at 37°C

(15 min. for pWOX5:GUS, 1h15 for pCYCA3;1CYCA3;1:GUS and 1h45 for pCYCB1;2:CYCB1;2:GUS), and subsequently stopped with ethanol (30% v/v, for 30 min at room temperature) and fixed for 30 min in FAA [Formaldehyde 5% (v/v), Acetic acid 10% (v/v), Ethanol 50% (v/v)] and finally overnight at 4°C in ethanol 70% before imaging with a Nikon SMZ1500 stereomicroscope equipped with a Nikon Digital Sight DS-5M camera. Quantification of GUS activity in pCYCB1;2:CYCB1;2:GUS was conducted by counting the blue spots (as described in Perilli and Sabatini, 2010) in GUS-stained pCYCB1;2:DB-CYCB1;2:GUS lines. To do so, microscope pictures were acquired serially across the root depth to account for all RAM cell layers, and cells were counted with FIJI cell counter Plugin.

To perform cell cycle synchronization, two week-old seedlings were transferred onto fresh solid Hoagland media + 2 mM hydroxyurea, and quickly put back in culture conditions (Cools *et al.*, 2010). At each time point, all seedlings from two plates containing both pCYCA3;1CYCA3;1:GUS and pCYCB1;2:CYCB1;2:GUS were harvested in cold acetone and GUS staining was performed as described above.

Ionome profiling

For each sample, seedlings from 48 plates, containing each 16 to 18 seedlings, were harvested after 24h or 48h of treatment, pooled and desorbed prior to ionome analysis as follows. The seedlings were washed twice in a desorption solution (5 mM CaCl₂, in 1 mM MES, pH5.7) for 10 min at 4°C and twice in distilled water (5 min, 4°C). About ~2 mm long root tips (RT) were then separated from the remaining root system (RR) with a clean scalpel blade on a clean surface. Dry root material was weighed into polytetrafluoroethylene digestion tubes and concentrated nitric acid [0.5 ml, 67-69 % (v/v)] was added to each tube. After 4 h incubation, samples were digested under pressure using a high-performance microwave reactor (Ultraclave 4, MLS). Digested samples were transferred to Greiner centrifuge tubes and diluted with de-ionized water. Elemental analysis was carried out using ICP-MS (Induced Coupled Plasma-Mass spectrometry analysis) [Sector Field High Resolution (HR)-ICP-MS, ELEMENT 2, Thermo Fisher Scientific]. For sample introduction a SC-2 DX Autosampler (ESI, Elemental Scientific) was used. A 6 points external calibration curve was set from a certified multiple standard solution (Bernd Kraft, Duisburg, Germany). Elements rhodium (Rh) and germanium (Ge) were infused online and used as internal standards.

For the *pad3* mutant characterization, samples were harvested after 11 days of growth under control, zinc excess (75 µM), and/or camalexin supplementation (250 nM) conditions on Hoagland agar plates.

Shoots and roots from 60 to 90 seedlings per sample were then pooled. The pooled roots were rinsed twice in a desorption solution (5 mM CaCl_2 , in 1 mM MES, pH 5.7) for 10 min at 4°C and twice in ultrapure Milli-Q water (Millipore) (5 min, 4°C). The pooled shoots were rinsed 5 min in ultrapure Milli-Q water (Millipore). Dried root and shoot samples (48h at 55°C) were weighed and digested in 1.5 mL of 65% HNO_3 by gradually heating (15 minutes at 45°C, 15 minutes at 65°C) up to 95°C for a 60-minute incubation. The digested samples were diluted to a final volume of 5 mL before analysis by ICP-OES (Inductively Coupled Plasma Optical Emission Spectroscopy) using a 5110 SVDV ICP-OES device (Agilent).

Laser Ablation ICP-MS

Roots were harvested and two regions of interest (ROI) along the primary roots were prepared: RAM (~200 μm from the tip of the columella) and differentiated roots (at a distance from the apex corresponding to 50 and 60% of root length). ROI of primary roots from several seedlings were aligned in a structure called “root bouquet” (Fig. S2). The portion of the bouquet containing either the aligned root tips or ROI of differentiated roots was dipped into liquid paraffin (42°C), dried for 3 s, re-dipped in liquid paraffin and placed in optimal cutting temperature media (OCT) in a rubber mold, before freezing in liquid nitrogen. At least seven 14 μm -thick perpendicular sections of the samples were cut in a cryotome (Leica CM050S, St. Gallen, Switzerland; precooled to -25°C), and transferred to microscopy glass slides, using Cryofilm 2C (SectionLab) as described in (Persson *et al.*, 2016). The first and last sections were used for fresh microscopy pictures, and the five middle sections were dried at -15°C (Fig. S2). The best dried section was photographed and selected for laser ablation ICP-MS (Fig. S2). Two bouquets were analyzed, as technical duplicates, for each condition and root part.

The Laser Ablation ICP MS system was composed of an Iridia Laser Ablation system (Teledyne CETAC Technologies, United Kingdom), coupled to a ICP-QQQ-MS 8900 instrument (Agilent, United Kingdom). Samples were digested at a spot size of 4 μm diameter, at 200 Hz, with a fluence of 0.5 $\text{J}\cdot\text{cm}^{-2}$. For the detection, three elements were analyzed; ^{39}K , ^{56}Fe and ^{66}Zn with integration times of 0.001, 0.01 and 0.07 s, respectively. The HDIP software was used for data analysis (Teledyne CETAC Technologies). Signal intensity across the root was taken by selecting a 20 μm -wide zone across all cell layers, as represented in Supplemental Fig. S2d-e, and used to represent signal over distance. With help of the HDIP software (Teledyne Photon Machine), the distance was cropped manually to each side of the roots, to exactly the external side of the epidermis. This distance was normalized to radius=1, and centered around 0.

RNA-Seq analysis

For RNA sequencing, a total of 48 plates containing 16-18 seedlings each were harvested per independent replicate per sample. RT samples were obtained by cutting at ~2 mm from the apex conducted, rapidly collected and frozen in liquid nitrogen (Fig. **S1**). RR tissues were also collected and frozen. Total RNA isolation was conducted with a Maxwell 16 device (Promega) using the Maxwell RSC Plant RNA Kit (Promega). RNA quality and concentration were measured with an Agilent 2100 Bioanalyzer Expert using the Agilent Nano 6000 Kit. Library preparation was performed with the TruSeq Stranded mRNA Sample Preparation Kit (Illumina), using 1 µg of total RNA as starting material. Library quality was assessed with a QIAxcel screening kit (Qiagen). Quantification, dilution and pooling of the libraries were done using the KAPA SYBR® FAST Universal qPCR Kit (Roche) and an Applied Biosystems 7900HT Real-Time PCR system. Sequencing (SE 100 nt) was done at the GIGA Genomics platform (University of Liège, Belgium) on a NextSeq500 device (Illumina) with standard workflow to obtain ~10-12 Mio reads/sample.

Data quality assessment and trimming were done with FastQC & Trimmomatic (Bolger *et al.*, 2014) with the following parameters: leading = 30, trailing =30, slidingwindow = 10:30, crop = 98, minlen =98. HiSAT2 was used for mapping on the *A. thaliana* genome [TAIR10 genome assembly and Araport11 annotation (Cheng *et al.*, 2017)]. Read counting was done with htseq-count (Anders *et al.*, 2015) and differential expression analysis with DESeq2 package (Love *et al.*, 2014). Calculation of differential expression between Zn excess samples and the corresponding control samples was realized with the following function and parameters: DESeq2::results(Def_DESeq, contrast, lfcThreshold = 1, alpha = 0.05), followed by padj < 0.05 and either log₂FoldChange > 1 or log₂FoldChange < -1 for selection of upregulated and downregulated genes, respectively.

GO enrichment analysis for biological processes was conducted with the Panther Database (<https://pantherdb.org/>) in September 2022, against *A. thaliana* annotated genes, with Bonferroni-correction with pval < 0.05. For graphical representation, GO represented by only one DEG were omitted, as well as two additional GO annotations which were too wide to provide useful information: *cellular process* (GO:0009987) and *biological_process* (GO:0008150).

RT-qPCR

Harvesting was carried out by separating the roots and shoots of 11-day-old seedlings, freezing them in liquid nitrogen and cold-grinding them twice using a ball mill at 30 Hz for 60 s (Retsch, Germany).

Samples were collected in triplicates of 40 to 50 seedlings. RNA was extracted using the NucleoSpin® RNA Plant Kit (Machery-Nagel, Germany), following the kit instructions. RNA quality and quantity were assessed by spectrophotometric analysis, and 1 µg was used for cDNA synthesis, using the RevertAid First Strand cDNA Synthesis Kit (Thermo Fisher Scientific, USA), according to the manufacturer instructions. RT-qPCR were performed on a QuantStudio™ 5 (Thermo Fisher Scientific, USA). Each reaction contained 5 µL of Takyon™ No ROX SYBR 2X MasterMix (Eurogentec, Belgium), 1 µL of 2.5 µM forward-reverse primer mix (Table S1) and 4 µL of 1:50 diluted cDNA. For amplification, cDNA was preincubated 2 min at 50°C, then 2 min at 95°C, followed by 40 cycles of 15 s at 95°C and 1 min at 60°C, and a final step of 15 s at 95°C, 1 min at 60 °C and 15 s at 95°C to determine dissociation curves. Data were analyzed using the Design & Analysis Software (v. 2.8.0, Thermo Fisher Scientific, USA), and qbase+ (v. 3.4.1, Biogazelle, Belgium). The analysis was done with three technical replicates for each sample/primer combination, and *UBIQUITIN10* (UBQ10), *EF1alpha* and *AT1G58050* were used as reference genes for data normalization.

Untargeted metabolomic analysis

For untargeted metabolomic analysis (Boutet *et al.*, 2022), plants were grown as described above. 48h after transferring seedlings to control or Zn excess plates, RT and RR samples were collected by cutting and collecting similar sized pieces of ~2 mm of RT and RR (~mid-distance from the apex).

Extraction of polar and semipolar primary and specialized metabolites. Metabolites were extracted from Arabidopsis root tissues by 2*1.8 mL of methanol:water:Acetone:Trifluoroacetic acid (30/28/42/0.1 V/V/V/V) and 500 ng of apigenin (Api, used as internal standard) were added to each sample. the supernatants were collected and dried using a speed vac before being resuspended in 200 µL of water and 10% acetonitrile for LC-MS/MS analysis.

Specialized metabolite extraction and UPLC-MS/MS analysis. Untargeted metabolomics data were acquired using a UHPLC system (Ultimate 3000 Thermo) coupled to quadrupole time of flight mass spectrometer (Q-ToF Impact II Bruker Daltonics, Bremen, Germany). For untargeted polar and semipolar metabolomic analysis, a Nucleoshell RP 18 plus reversed-phase column (2 x 100 mm, 2.7 µm; Macherey-Nagel) was used for chromatographic separation. The mobile phases used for the chromatographic separation were (A) 0.1% formic acid in H₂O and (B) 0.1% formic acid in acetonitrile. The flow rate was of 400 µL/min and the following gradient was used: 95% of A for 1-min, followed by a linear gradient from 95% A to 80% A from 1 to 3-min, then a linear gradient from 80% A to 75% A from 3 to 8-min, a linear gradient from 75% A to 40% A from 8 to 20-min. 0% of A was hold until 24-min, followed by a linear

gradient from 0% A to 95% A from 24 to 27-min. Finally, the column was washed by 30% A at for 3.5-min then re-equilibrated for 3.5-min (35-min total run time). Data-dependent acquisition (DDA) methods were used for mass spectrometer data in positive and negative ESI modes using the following parameters: capillary voltage, 4.5kV; nebulizer gas flow, 2.1 bar; dry gas flow, 6 L/min; drying gas in the heated electrospray source temperature, 140°C. Samples were analyzed at 8 Hz with a mass range of 100 to 1500 m/z. Stepping acquisition parameters were created to improve the fragmentation profile with a collision RF from 200 to 700 Vpp, a transfer time from 20 to 70 μ s and collision energy from 20 to 40 eV. Each cycle included a MS fullscan and 5 MS/MS CID on the 5 main ions of the previous MS spectrum.

Metabolomic data processing. The .d data files (Bruker Daltonics, Bremen, Germany) were converted to .mzXML format using DataAnalysis from Bruker Daltonics. mzXML data processing, mass detection, chromatogram building, deconvolution, samples alignment, and data export, were performed using the MZmine 2.52 software (<http://mzmine.github.io/>) for both positive and negative data files. The ADAP chromatogram builder (Myers *et al.*, 2017) method was used with a minimum group size of scan 5, a group intensity threshold of 5000, a minimum highest intensity of 5000 and m/z tolerance of 10 ppm. Deconvolution was performed with the ADAP wavelets algorithm using the following setting: S/N threshold 8, peak duration range = 0.01-2.1 min retention time wavelet range 0.0-0.05 min, MS2 scan were paired using a m/z tolerance range of 0.2 Da and retention time tolerance of 0.2 min. Then, isotopic peak grouper algorithm was used with a m/z tolerance of 10 ppm and retention time tolerance of 0.5. All the peaks were filtered using feature list row filter keeping only peaks with MS2 scan. The alignment of samples was performed using the join aligner with an m/z tolerance of 10 ppm, a weight for m/z and retention time at 1, a retention time tolerance of 0.5 min. First research in library with Mzmine was done with identification module and “custom database search” to begin the annotation with our library, currently containing 103 annotations (retention time and m/z) in positive mode and 67 in negative mode, with retention time tolerance of 0.3 min and m/z tolerance of 0.0025 Da or 6 ppm.

Molecular networking. Molecular networks were generated with MetGem software (Olivon *et al.*, 2018; <https://metgem.github.io>) using the .mgf and .csv files obtained with MZmine2 analysis. The molecular network was optimized for the ESI+ and ESI- datasets and different cosine similarity score thresholds were tested. ESI- and ESI+ molecular networks were generated using cosine score thresholds of 0.8, in positive mode and negative mode. Optimal parameters that allowed a good cluster separation among metabolites were set up.

Metabolite annotations. Metabolite annotations were performed in four consecutive steps. First, the obtained RT and m/z data of each feature were compared with our home-made library containing more than 150 standards or experimental common features (retention time, m/z). Second, the ESI- and ESI+ metabolomic data used for molecular network analyses were searched against the available MS2 spectral libraries (Massbank NA, GNPS Public Spectral Library, NIST14 Tandem, NIH Natural Product and MS-Dial), with absolute m/z tolerance of 0.02, 4 minimum matched peaks and minimal cosine score of 0.65. Third, not-annotated metabolites that belong to molecular network clusters containing annotated metabolites from step 1 and 2 were assigned to the same chemical family. Finally, for metabolites that had no or unclear annotation, the Sirius software (<https://bio.informatik.uni-jena.de/software/sirius/>) was used. Sirius is based on machine learning techniques that use available chemical structures with the CANOPUS module (Dührkop *et al.*, 2021) and MS/MS data from chemical databanks to propose structures of unknown compounds.

Metabolite normalization. Considering (i) the small size of the samples and the difficulty of weighting them, and (ii) the very different total abundances of metabolites between the two root parts (6 times more abundant in RR than RT, Fig. **S11b**), two methods of data normalization were considered : (i) normalization according to the number of collected root parts (Fig. **S11a,b**), and (ii) normalization according to the total metabolite abundance in each sample (Fig. **6a**). The two methods differently impacted how the variance was partitioned among root part (78% vs 57%, respectively) and treatment (13% vs 18%, respectively) (Fig. **S11a**, Fig. **6a**). As this method provides consistent total metabolite abundance across samples, which facilitates reliable comparisons, and is commonly used in the literature (Holmes *et al.*, 2008; Di Guida *et al.*, 2016; Pang *et al.*, 2022), data were normalized by the total count of control samples, enabling a detailed analysis of the impact of the treatment in each root part.

Targeted camalexin analysis

Camalexin extraction was adapted from Tewes *et al.* (2018). Upon harvest, roots and shoots from 11 day-old Col-0 and *pad3-3* seedlings were separated, then weighted (100 to 500 mg) and frozen in liquid nitrogen. Plant material was then frozen ground using a ball mill at 30 Hz for 60 s, twice (Retsch, Germany). A first camalexin extraction was performed using 400 to 500 µL of 80 % (v/v) HPLC grade methanol (Sigma Aldrich, USA). Samples were homogenized and incubated for 10 min at 60°C and 1000 rpm in a reaction block (Thermomixer, Eppendorf, Germany). Samples were centrifuged at room temperature for 5 min at 17 000 g. The supernatant was collected in a new tube and the extraction

operation was repeated a second time. The two joined supernatants were dried under reduced pressure with a RVC 2-33 CDplus (Christ, Germany). Samples were resuspended in 200 to 1000 μL of 80 % methanol, filtered through a polytetrafluoroethylene (PTFE) membrane filter and analyzed using Ultra-Performance Liquid Chromatography–High-Resolution Mass Spectrometry (UPLC-HRMS).

The UPLC-HRMS analyses were performed on a Waters ACQUITY Ultra Performance LC system equipped with a Waters Synapt XS Q-TOF. A 5.0 μL sample solution was injected for each run. Chromatographic separation was performed with a flow of 0.5 ml/min, at 40°C, using the 1.7 μm ACQUITY UPLC BEH C18 Column (2.1 mm X 50 mm dimension, 130 Å pores). The mobile phase consisted of water (containing 0.1% formic acid – solvent A) and acetonitrile (containing 0.1% formic acid – solvent B). The elution gradient was 0 - 1 min, 5% B; 1.0 - 25.0 min, 5 - 100% B; 25.0 - 28.0 min, 100% B; 28.0 - 28.5 min, 100.0 - 5.0% B; 28.5- 30.0 min, 5.0% B. UV spectra was recorded with the built-in ACQUITY UPLC Photodiode Array (PDA) detector with a wavelength ranging from 190 to 500 nm, resolution of 1.2 nm and a sampling rate of 20 points/sec. Mass spectrometry analyses were performed on positive electrospray polarity with a source temperature of 150°C. The capillary and cone voltage were set at 0.5 kV and 70 V, respectively. An MSe continuum function in resolution mode with an extended dynamic range, a scan range of 50 to 1200 m/z and a scan time of 0.15 seconds was used. For the high energy (MS2) data collection a collision energy ramp from 20 to 70 V was set for the transfer cell. All mass spectrometry analyses were acquired using Leucine-enkephalin solution (100 ng/ml in $\text{H}_2\text{O}/\text{ACN}$ 50:50) as the internal calibrant. All LC-MS data analysis was performed on Masslynx V 4.2 SCN1015. Lockspray correction was performed based on the calculated monoisotopic mass of the $\text{M}+\text{H}^+$ ion of Leucine-enkephalin (556.2766).

Camalexin was identified based on the retention time of an external standard of commercial camalexin (Sigma-Aldrich), and the identity was confirmed based on the m/z value of camalexin's $[\text{M}+\text{H}]$ adduct detected on the mass spectra (mass error lower than 5 ppm). For camalexin quantification, Extracted Ion Chromatograms (EIC) for camalexin's $[\text{M}+\text{H}]$ ion was generated for seven standard camalexin solutions (0.0 μM , 0.05 μM , 0.2 μM , 0.5 μM , 1.0 μM , 2.0 μM , 3.0 μM , 5.0 μM) from which peak area was calculated and used to construct a calibration curve. Concentration was then reported per gram of fresh weight.

References

- Anders S, Pyl PT, Huber W. 2015.** HTSeq-A Python framework to work with high-throughput sequencing data. *Bioinformatics* **31**: 166–169.
- Bolger AM, Lohse M, Usadel B. 2014.** Trimmomatic: A flexible trimmer for Illumina sequence data. *Bioinformatics* **30**: 2114–2120.
- Böttcher C, Chapman A, Fellermeier F, Choudhary M, Scheel D, Glawischnig E. 2014.** The biosynthetic pathway of indole-3-carbaldehyde and indole-3-carboxylic acid derivatives in arabidopsis. *Plant Physiology* **165**: 841–853.
- Böttcher C, Westphal L, Schmotz C, Prade E, Scheel D, Glawischnig E. 2009.** The multifunctional enzyme CYP71b15 (Phytoalexin deficient3) converts cysteine-Indole-3-acetonitrile to camalexin in the Indole-3-acetonitrile metabolic network of *Arabidopsis thaliana*. *Plant Cell* **21**: 1830–1845.
- Cheng CY, Krishnakumar V, Chan AP, Thibaud-Nissen F, Schobel S, Town CD. 2017.** Araport11: a complete reannotation of the *Arabidopsis thaliana* reference genome. *Plant Journal* **89**: 789–804.
- Cools T, Iantcheva A, Maes S, Van den Daele H, De Veylder L. 2010.** A replication stress-induced synchronization method for *Arabidopsis thaliana* root meristems. *The Plant Journal* **64**: 705–714.
- Dührkop K, Nothias LF, Fleischauer M, Reher R, Ludwig M, Hoffmann MA, Petras D, Gerwick WH, Rousu J, Dorrestein PC, et al. 2021.** Systematic classification of unknown metabolites using high-resolution fragmentation mass spectra. *Nature Biotechnology* **39**: 462–471.
- Glazebrook J, Zook M, Mert IF, Kagan I, Rogers EE, Crute IR, Holub EB, Hammerschmidt R, Ausubelt FM. 1997.** Phytoalexin-Deficient Mutants of *Arabidopsis* Reveal That *PAD4* Encodes a Regulatory Factor and That Four *PAD* Genes Contribute to Downy Mildew Resistance. *Genetics* **146**: 381–392.
- Di Guida R, Engel J, Allwood JW, Weber RJM, Jones MR, Sommer U, Viant MR, Dunn WB. 2016.** Non-targeted UHPLC-MS metabolomic data processing methods: a comparative investigation of normalisation, missing value imputation, transformation and scaling. *Metabolomics : Official journal of the Metabolomic Society* **12**.
- Holmes E, Loo RL, Stamler J, Bictash M, Yap IKS, Chan Q, Ebbels T, De Iorio M, Brown IJ, Veselkov KA, et al. 2008.** Human metabolic phenotype diversity and its association with diet and blood pressure. *Nature* **453**: 396–400.
- Hornbacher J, Horst-Niessen I, Herrfurth C, Feussner I, Papenbrock J. 2022.** First experimental evidence suggests use of glucobrassicin as source of auxin in drought-stressed *Arabidopsis thaliana*. *Frontiers in Plant Science* **13**: 1–17.

Kriechbaumer V, Wang P, Hawes C, Abell BM. 2012. Alternative splicing of the auxin biosynthesis gene YUCCA4 determines its subcellular compartmentation. *Plant Journal* **70**: 292–302.

Love MI, Huber W, Anders S. 2014. Moderated estimation of fold change and dispersion for RNA-seq data with DESeq2. *Genome Biology* **15**: 1–21.

Mikkelsen MD, Naur P, Halkier BA. 2004. Arabidopsis mutants in the C-S lyase of glucosinolate biosynthesis establish a critical role for indole-3-acetaldoxime in auxin homeostasis. *Plant Journal* **37**: 770–777.

Mucha S, Heinzlmeir S, Kriechbaumer V, Strickland B, Kirchhelle C, Choudhary M, Kowalski N, Eichmann R, Hückelhoven R, Grill E, et al. 2019. The Formation of a Camalexin Biosynthetic Metabolon. *The Plant cell* **31**: 2697–2710.

Myers OD, Sumner SJ, Li S, Barnes S, Du X. 2017. One Step Forward for Reducing False Positive and False Negative Compound Identifications from Mass Spectrometry Metabolomics Data: New Algorithms for Constructing Extracted Ion Chromatograms and Detecting Chromatographic Peaks. *Analytical Chemistry* **89**: 8696–8703.

Nafisi M, Goregaoker S, Botanga CJ, Glawischnig E, Olsen CE, Halkier BA, Glazebrook J. 2007. Arabidopsis cytochrome P450 monooxygenase 71A13 catalyzes the conversion of indole-3-acetaldoxime in camalexin synthesis. *Plant Cell* **19**: 2039–2052.

Olivon F, Elie N, Grelier G, Roussi F, Litaudon M, Touboul D. 2018. MetGem Software for the Generation of Molecular Networks Based on the t-SNE Algorithm. *Analytical chemistry* **90**: 13900–13908.

Pang Z, Zhou G, Ewald J, Chang L, Hacariz O, Basu N, Xia J. 2022. Using MetaboAnalyst 5.0 for LC–HRMS spectra processing, multi-omics integration and covariate adjustment of global metabolomics data. *Nature Protocols* **2022 17:8 17**: 1735–1761.

Pastorczyk M, Kosaka A, Piślewska-Bednarek M, López G, Frerigmann H, Kułak K, Glawischnig E, Molina A, Takano Y, Bednarek P. 2020. The role of CYP71A12 monooxygenase in pathogen-triggered tryptophan metabolism and Arabidopsis immunity. *New Phytologist* **225**: 400–412.

Perilli S, Sabatini S. 2010. Analysis of Root Meristem Size Development. *Plant Developmental Biology: Methods and Protocols* **655**: 177–187.

Persson DP, Chen A, Aarts MGM, Salt DE, Schjoerring JK, Husted S. 2016. Multi-element bioimaging of *Arabidopsis thaliana* roots. *Plant Physiology* **172**: 835–847.

Pfalz M, Mikkelsen MD, Bednarek P, Olsen CE, Halkier BA, Kroymann J. 2011. Metabolic engineering in *Nicotiana benthamiana* reveals key enzyme functions in Arabidopsis indole glucosinolate modification.

Plant Cell **23**: 716–729.

Pfalz M, Mukhaimar M, Perreau F, Kirk J, Hansen CIC, Olsen CE, Agerbirk N, Kroymann J. 2016. Methyl transfer in glucosinolate biosynthesis mediated by indole glucosinolate O-methyltransferase 5. *Plant Physiology* **172**: 2190–2203.

Rajniak J, Barco B, Clay NK, Sattely ES. 2015. A new cyanogenic metabolite in *Arabidopsis* required for inducible pathogen defence. *Nature* **525**: 376–379.

Richtmann L, Thiebaut N, Sarthou M, Ranjan A, Boutet S, Hanikenne M, Verbruggen N, Clemens S. 2024. A multi-omics analysis of *Arabidopsis thaliana* root tips under Cd exposure: A role of HY5 in limiting accumulation. *bioRxiv*: doi:10.1101/2024.08.29.609871.

Sønderby IE, Geu-Flores F, Halkier BA. 2010. Biosynthesis of glucosinolates - gene discovery and beyond. *Trends in Plant Science* **15**: 283–290.

Tewes LJ, Stolpe C, Kerim A, Krämer U, Müller C. 2018. Metal hyperaccumulation in the Brassicaceae species *Arabidopsis halleri* reduces camalexin induction after fungal pathogen attack. *Environmental and Experimental Botany* **153**: 120–126.